

Determination of Magnetic Fields in a Plasma from the Contour of Hydrogen Spectral Lines

A. V. Demura and V. S. Lisitsa

I. V., Kurchatov Institute of Atomic Energy

Submitted December 24, 1971

Zh. Eksp. Teor. Fiz. 62, 2161-2169 (June 1972)

An approximate analytic solution is obtained for the problem of deformation of the Holtsmark contour of a hydrogen spectral line by an external magnetic field B . This solution makes it possible to obtain the difference contour, determined by subtracting two contours corresponding to polarization parallel and perpendicular to the magnetic field. A method of determining the magnitude and direction of B with the aid of this difference contour, expressed in terms of three universal functions connected with the Holtsmark function, is considered. Numerical results are given for the components of the lines L_α and L_β . The possibility of finding the exact analytic solution for the complete line contour is discussed.

1. INTRODUCTION

THE determination of the magnetic field in a plasma with the aid of spectroscopic measurements is of great practical interest^[1]. Such measurements are preferable because they do not call for external objects to be introduced into the plasma. There is a well known method of determining the magnetic fields from the Zeeman structure of atomic lines (cf., e.g.,^[1,2]). At the same time, in a large number of experiments the Zeeman structure of the level is not clearly pronounced. This pertains in particular to the case of sufficiently high densities in a hydrogen plasma (for example, installations of the plasma-focus or magnetic-piston type), when the Zeeman structure turns out to be almost completely smeared out because of the linear Stark effect in the ion fields. In this case it is practically impossible to determine the magnetic fields by measuring the Zeeman effect.

Under the described conditions, the line profile is the result of the joint interaction of the atom with the magnetic field B and with the plasma microfield F . This complicates greatly the calculation of the line contour. Whereas in the absence of B the problem reduces to well-known analytic results^[3], corresponding line-contour calculations for $B \neq 0$ have been published only very recently^[4] and reduce essentially to the development of certain computer-solution algorithms. Yet it is of undisputed interest to obtain sufficiently simple analytic solutions of this problem, since they would greatly simplify the interpretation of spectroscopic data, thereby increasing their reliability. We derive below such analytic solutions for definite regions of the line contour, and propose on their basis a method for determining the magnitudes and directions of the magnetic fields.

2. POLARIZATION CHARACTERISTIC

We consider the influence of a homogeneous constant magnetic field B on the static-Holtsmark profile of hydrogen spectral lines (see^[3])¹⁾. We recall that the problem of determining the magnetic field is vital for

¹⁾Here, just as in^[4], it is assumed that the influence of the magnetic field on the character of the plasma-particle collisions can be neglected, i.e., that the condition $r_L \gg r_D$ is satisfied, where r_L and r_D are the Larmor and Debye radii of the ions. The action of the plasma electrons can be easily taken into account by functional convolution of the obtained contour with the electron impact contour, cf.^[4].

the case when the Zeeman structure is "smeared out." A simple estimate of the ratio of the Zeeman splitting $\Delta E_Z = (n-1)\mu_0 B$ (n is the principal quantum number and $\mu_0 = e\hbar/2mc$ is the Bohr magneton) to the Stark splitting $\Delta E_S = \frac{3}{2}n(n-1)e a_0 F_0$ (a_0 is the Bohr radius, $F_0 = 2.6eN^{2/3}$ is the "normal" Holtsmark field, and N is the ion concentration in the plasma) yields

$$\frac{\Delta E_Z}{\Delta E_S} = \frac{1}{3n} \frac{e^2 B}{\hbar c F_0} \approx 1.95 \cdot 10^6 n^{-1} B N^{-2/3}, \quad (1)$$

where B is in gauss and N in cm^{-3} . For example, for fields $B \sim 10^6$ G and concentrations $N \sim 10^{18} \text{ cm}^{-3}$ this ratio is of the order of unity for $n = 2$.

We consider below the case when the parameter (1) is small (a more rigorous criterion will be derived from the final result in Sec. 4). The corresponding calculations are based on a successive application of perturbation theory with respect to this parameter. Naturally, the line-contour corrections obtained in this manner are small compared with the zeroth (Holtsmark) approximation. The calculated correction, however, being connected with the magnetic field, reflects different properties of radiation polarized along and across the magnetic field. These properties can be revealed with the aid of the polarization characteristic usually employed in experiments on the polarization of radiation in the excitation of atoms^[5]:

$$\Pi = (I_{\parallel} - I_{\perp}) / (I_{\parallel} + I_{\perp}), \quad (2)$$

where I_{\parallel} and I_{\perp} are the profiles of the emission line polarized parallel and perpendicular to B when observed in a direction perpendicular to B . The difference $I_{\parallel} - I_{\perp}$ in (2) does not contain a "zeroth" unpolarized radiation and is therefore completely determined by corrections containing the magnetic field. Thus, the problem reduces to calculating the corrections for the radiation polarized parallel and perpendicular to B , followed by calculation of the difference contour $I_{\parallel} - I_{\perp}$.

To a certain degree, this situation is analogous to the devices used to calculate the asymmetry of the Stark contours for hydrogen^[6]. We note that in this case the attained measurement accuracy is of the order of 1% ^[7]. The fruitfulness of using approaches of this type is confirmed also by recent experiments on the anisotropy of ion-acoustic noise in a turbulent plasma^[8].

The case of Zeeman-Stark broadening entails much greater computational difficulties than, say, the case of Zeeman-Doppler broadening, where the determination B

is quite simple, cf. [1]. We shall therefore disregard henceforth the Doppler effect, as can be done when $T[\text{eV}] < 10^{-2} \lambda_0^{2/3} n(n-1) \hbar/m^2 N^{4/3}$ (T is the temperature of the atoms and λ_0 is the wavelength in Å). We note that for the line wing the Stark mechanism remains decisive even if this inequality is noticeably violated.

3. DIFFERENCE LINE CONTOUR

The quasiclassical profile $I(\omega)$ of the component of the atom line is given by

$$I_{ij}(\omega) = \{ |\langle \Psi_i | \mathbf{d} e | \Psi_j \rangle|^2 \delta(\Delta\omega - \Delta E/\hbar) \}_{\text{av}}, \quad (3)$$

where $\Psi_{i,f}$ are the wave functions of the initial and final states of the atom, \mathbf{d} is the atom dipole-moment vector, \mathbf{e} is the radiation-polarization vector, ΔE is the change of the energy as a result of the perturbation, $\Delta\omega = \omega - \omega_0$; ω and ω_0 are the observed and unperturbed transition frequencies, and the symbol $\{ \dots \}_{\text{av}}$ denotes averaging over the Holtsmark distribution of the fields.

We choose a coordinate system that is stationary in space with axis $Z \parallel \mathbf{B}$. We specify the direction of the vector \mathbf{F} with the aid of the Euler angles θ and ψ (see Fig. 1). Then the Schrödinger equation for the hydrogen atom becomes

$$\left(\hat{H}_0 - d\mathbf{F} - \frac{e\hbar}{2mc} \hat{L}_z \mathbf{B} \right) \Psi = E\Psi, \quad (4)$$

where H_0 is the unperturbed Hamiltonian of the atom, \hat{L} is the orbital-momentum operator, and E is the eigenvalue of the energy.

It is assumed, as in [4], that the Paschen-Back effect takes place, so that we can disregard in the calculations the electron spin (allowance for it would shift the energy of each level by $\pm e\hbar\mathbf{B}/2mc$, depending on the sign of the projection of \mathbf{S} on \mathbf{B}).

To determine the eigenfunctions and the eigenvalues of (4), we use perturbation theory. The zeroth-approximation wave functions are chosen to be the Stark wave functions $\Psi_{n_1 n_2 m}$ in the coordinate system with $Z' \parallel \mathbf{F}$ (Fig. 1), in contrast to the usual choice of the spherical functions Ψ_{nlm} (cf. [4]). This makes it unnecessary to solve the secular equations and by the same token enables us to use the formulas of perturbation theory without degeneracy for the interaction $\hat{V} \equiv e\hbar L_z \mathbf{B}/2mc$. It should be noted, however, that the procedure in question has a definite peculiarity, namely, the wave functions $\Psi_{n_1 n_2 m}$ are taken in a coordinate system connected with the field \mathbf{F} , while the polarization characteristic is taken in the coordinate system connected with the field \mathbf{B} . We introduce the symbol \hat{R} for the rotation

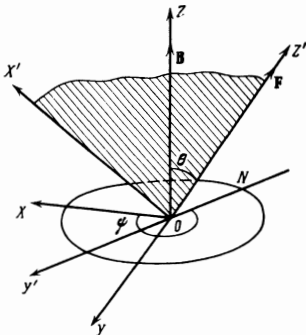


FIG. 1. Position of the coordinate system $X'Y'Z'$ connected with the field \mathbf{F} relative to the laboratory system XYZ . The Z and Z' are directed along the vectors \mathbf{B} and \mathbf{F} , the angle between which is θ ; the Y' axis lies in the XOY plane; ψ is the angle between the X axis and the node line N .

operator that makes these coordinate systems congruent. Then the perturbation-theory series for the energy and the eigenfunctions take the following form, with accuracy up to terms of second order inclusive;

$$\Delta E_k \approx \Delta E_k^{(0)} + \Delta E_k^{(1)} + \Delta E_k^{(2)} = \hbar \frac{\alpha}{e} q_k F_0 \left\{ 1 + \frac{\epsilon B}{q_k F_0} \times \langle k | \hat{R}^+ \hat{L}_z \hat{R} | k \rangle + \left(\frac{\epsilon B}{q_k F_0} \right)^2 \sum_{m \neq k} \frac{|\langle \hat{R}^+ \hat{L}_z \hat{R} \rangle_{km}|^2}{1 - q_m/q_k} \right\}, \quad (5)$$

$$\Psi_k \approx \Psi_k^{(0)} + \Psi_k^{(1)} + \Psi_k^{(2)} = \Psi_k^{(0)} + \frac{\epsilon B}{q_k F_0} \sum_{m \neq k} \frac{(\hat{R}^+ \hat{L}_z \hat{R})_{mk}}{1 - q_m/q_k} \Psi_m^{(0)} + \left(\frac{\epsilon B}{q_k F_0} \right)^2 \sum_{m \neq k} \left\{ \sum_{n \neq k} \frac{(\hat{R}^+ \hat{L}_z \hat{R})_{mn} (\hat{R}^+ \hat{L}_z \hat{R})_{nk}}{(1 - q_n/q_k)(1 - q_m/q_k)} \Psi_m^{(0)} - \frac{(\hat{R}^+ \hat{L}_z \hat{R})_{kk} (\hat{R}^+ \hat{L}_z \hat{R})_{mk}}{(1 - q_m/q_k)^2} \Psi_m^{(0)} - \frac{1}{2} \frac{(\hat{R}^+ \hat{L}_z \hat{R})_{kk}^2}{(1 - q_m/q_k)} \Psi_k^{(0)} \right\}, \quad (6)$$

where $q_k = n_{1k} - n_{2k}$ is the difference between the parabolic quantum numbers of the given state k , $\alpha = 3ne^2 a_0 / 2\hbar$, $\epsilon \equiv e^2 / 3\hbar c$, $\Psi_k^{(0)} \equiv \Psi_{n_1 k n_2 k m k}$. The action of the operator \hat{R} is given by the formulas [9]

$$\hat{R}^+ \hat{A}_x \hat{R} = (\hat{A}_{x'} \sin \theta - \hat{A}_x \cos \theta) \sin \psi - \cos \psi \hat{A}_{y'}, \quad (7)$$

$$\hat{R}^+ \hat{A}_z \hat{R} = \hat{A}_z \cos \theta + \hat{A}_x \sin \theta,$$

where \mathbf{A}_Z and \mathbf{A}_X are specified in the coordinate system connected with the field \mathbf{B} , and $\mathbf{A}_{X'}$, $\mathbf{A}_{Y'}$, and $\mathbf{A}_{Z'}$ in the system connected with the field \mathbf{F} . We use for the δ -function in (3) the expansion

$$\delta \left(\Delta\omega - \frac{\Delta E}{\hbar} \right) \approx \delta \left(\Delta\omega - \frac{\Delta E^{(0)} + \Delta E^{(1)} + \Delta E^{(2)}}{\hbar} \right) \approx \delta \left(\Delta\omega - \frac{\Delta E^{(0)}}{\hbar} \right) - \frac{\Delta E^{(1)}}{\hbar} \delta' \left(\Delta\omega - \frac{\Delta E^{(0)}}{\hbar} \right) - \frac{\Delta E^{(2)}}{\hbar} \delta' \left(\Delta\omega - \frac{\Delta E^{(0)}}{\hbar} \right) + \frac{1}{2} \left(\frac{\Delta E^{(1)}}{\hbar} \right)^2 \delta'' \left(\Delta\omega - \frac{\Delta E^{(0)}}{\hbar} \right). \quad (8)$$

Assuming for simplicity that the state Ψ_f is unperturbed, substituting (5)–(8) in (3), and combining terms of like order of smallness in $\epsilon B/q_k F_0$, we obtain an expression for the profile of the component with polarization \mathbf{e} . Assuming $\mathbf{e} \parallel Z$ and $\mathbf{e} \parallel X$, we obtain expressions for the profiles $I^Z(\omega)$ and $I^X(\omega)$ of the components with polarization along the Z and X axes, respectively. Setting up furthermore the difference contour $I^{Z-X}(\omega) = I^Z(\omega) - I^X(\omega)$, averaging over the angles with allowance for (7), and going over to the dimensionless contour $I(\beta)$, defined by the relation

$$I(\omega) d\omega = |d_{if}|^2 I(\beta) d\beta \quad (\beta \equiv (\omega - \omega_0) / \alpha e^{-1} q_k F_0),$$

we get

$$I_h^{i-x}(\beta) \approx \left(\frac{\epsilon B}{q_k F_0} \right)^2 \left\{ C_{1k}^{i-x} \frac{\mathcal{H}(\beta)}{\beta^2} + C_{2k}^{i-x} \frac{d}{d\beta} \left[\frac{\mathcal{H}(\beta)}{\beta} \right] + C_{3k}^{i-x} \frac{d^2}{d\beta^2} [\mathcal{H}(\beta)] \right\}, \quad (9)$$

where C_{lk}^{Z-X} are numerical coefficients determined by the sums from (5) and (6), and $l = 1, 2, 3$; the explicit form of C_{lk}^{Z-X} is given in the Appendix; $\mathcal{H}(\beta)$ is the Holtsmark function [11].

We see thus that the difference contour for any line is proportional to the square of the magnetic field and is expressed in terms of the three universal functions $f_1 \equiv \mathcal{H}(\beta)/\beta^2$, $f_2 \equiv d(\beta^{-1}\mathcal{H}(\beta))/d\beta$, $f_3 \equiv d^2\mathcal{H}(\beta)/d\beta^2$, the values of which are given in the table.

β	$f_1(\beta)$	$f_2(\beta)$	$f_3(\beta)$	β	$f_1(\beta)$	$f_2(\beta)$	$f_3(\beta)$
0.0	0.4240	0.4244	0.8488	2.4	0.0473	-0.1198	-0.0087
0.2	0.4170	0.4012	0.7561	2.6	0.0352	-0.1004	0.0489
0.4	0.3940	0.3365	0.5092	2.8	0.0262	-0.0820	0.0805
0.6	0.3600	0.2428	0.1780	3.0	0.0196	-0.0657	0.0930
0.8	0.3175	0.1373	-0.1482	3.4	0.0110	-0.0410	0.0851
1.0	0.2712	0.0365	-0.3956	4.0	0.0050	-0.0199	0.0542
1.2	0.2248	-0.0469	-0.5259	4.4	0.0035	-0.0126	0.0369
1.4	0.1815	-0.1063	-0.5366	5.0	0.0016	-0.0063	0.0203
1.6	0.1431	-0.1408	-0.4655	5.5	0.0010	-0.0041	0.0126
1.8	0.1106	-0.1539	-0.3441	6.0	0.0006	-0.0026	0.0081
2.0	0.0842	-0.1509	-0.2125	6.5	0.0005	-0.0017	0.0053
2.2	0.0534	-0.1379	-0.0965	7.0	0.0003	-0.0012	0.0036

The coefficients C_{lk}^{Z-X} were calculated for the concrete lines using the general formulas for the matrix elements of the operator \hat{L} in parabolic coordinates obtained on the basis of the four-dimensional symmetry properties of the hydrogen atom (cf., e.g., [12]). The matrix elements of the operator \hat{d} were taken from [13].

4. DIFFERENCE CONTOUR OF L_α AND L_β

The calculation described above gives for the side component $100 \rightarrow 000$ of the L_α line the following result:

$$I_{(100)}^{Z-X} \approx \left(\frac{\epsilon B}{F_0}\right)^2 \left\{ -\frac{11}{15} \frac{\mathcal{H}(\beta)}{\beta^2} + \frac{1}{15} \frac{d}{d\beta} \left[\frac{\mathcal{H}(\beta)}{\beta} \right] \right\}. \quad (10)$$

It can be verified that this result agrees with the corresponding expression that can be derived from [4] by series expansion of the intermediate analytic formulas (44) of [4] for the particular case of L_α .

For the side component $101 \rightarrow 000$ of the L_β line we obtain

$$I_{(101)}^{Z-X} \approx \left(\frac{\epsilon B}{F_0}\right)^2 \left\{ 8 \frac{\mathcal{H}(\beta)}{\beta^2} - \frac{12}{5} \frac{d}{d\beta} \left[\frac{\mathcal{H}(\beta)}{\beta} \right] - \frac{4}{5} \frac{d^2}{d\beta^2} [\mathcal{H}(\beta)] \right\}. \quad (11)$$

The contours (10) and (11) are shown in Fig. 2.

The condition for the applicability of the results is obviously the requirement that the difference contour be small in comparison with the Holtmark contour

$$\mathcal{H}(\beta) \gg I^{Z-X}(\beta). \quad (12)$$

Using the well known limiting expressions for $\mathcal{H}(\beta)$ in the cases $\beta \gg 1$ and $\beta \ll 1$, we obtain for $I^{Z-X}(\beta)$:

$$I^{Z-X}(\beta) = \begin{cases} \left(\frac{\epsilon B}{F_0}\right)^2 \frac{1.5}{\beta^{3/2}} \left(C_{1a} - \frac{7}{2} C_{2a} + \frac{35}{4} C_{3a} \right), & \beta \gg 1 \\ \left(\frac{\epsilon B}{F_0}\right)^2 \frac{3}{4\pi} (C_{1a} + C_{2a} + 2C_{3a}), & \beta \ll 1 \end{cases} \quad (13)$$

Substituting (13) in (12), we obtain for $\beta \gg 1$ the condition

$$\beta \gg \epsilon B / F_0. \quad (14)$$

and a condition of similar form for $\beta \ll 1$.

Formulas (12) and (14) are rigorous criteria for the applicability of the described approach. An analysis of these formulas shows that the results obtained above cover a rather wide range of experimental conditions. In fact, the necessary requirement that the obtained correction (12) and (14) be small can be satisfied for a given value of B by many different methods, such as going over to higher line, increasing the concentration, and a transition to the line wing. We note that the contours (10) and (11) do not satisfy the requirement of normalization at zero, since these results do not hold, according to (14), in the immediate vicinity of the line center.

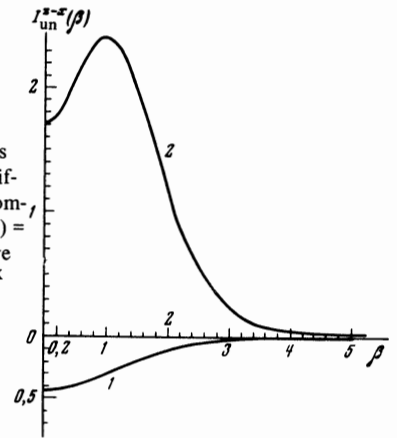


FIG. 2. Universal functions $I_{un}^{Z-X}(\beta)$, which determine the difference contours of the line components: $100 \rightarrow 000 L_\alpha (I_{un}^{Z-X}(\beta) = (15/11)I^{Z-X}(\beta)/(\epsilon B/F_0)^2$ - curve 1), $101 \rightarrow 000 L_\beta (I_{un}^{Z-X}(\beta) = I^{Z-X}(\beta)/(\epsilon B/F_0)^2$ - curve 2).

It is of interest to compare the analytic results with the numerical data [4]. These data (which include also electronic impact broadening) are represented in the form of extensive tables of the line contours for observation along and across the magnetic field. Using formulas (36) and (37) of [4] we can verify that the difference contour corresponding to the two indicated observation directions coincide with the one introduced above (see (9)). When it comes to a direct comparison with [4], several difficulties arise, connected mainly with the fact that the comparison must be made for difference-contour values that are, on the one hand, quite small (when the results of (9) are already valid), and on the other hand large enough and exceed the error of the numerical calculation ($\sim 1\%$ in [4]); in addition, it is necessary to be far enough away from the line center to decrease the influence of the electron impact broadening, which is taken into account in [4,2]. When the indicated conditions are satisfied, say, for the line L_α at a density $N \sim 10^{16} \text{ cm}^{-3}$, the two difference contours agree (within $\sim 20\%$) for fields $B = 20, 40,$ and 60 kG in the region from $\beta \sim 1$ (at $B = 20 \text{ kG}$) and from $\beta \sim 2$ (for $B = 40$ and 60 kG). Thus, the influence of the magnetic field B is described by the result (9), which determines the value of B directly, already at a distance of half the line width away from the line center.

The results enable us to extract information not only on the magnitude but also on the direction of the magnetic field. In fact, the effect calculated above is connected with the coordinate system oriented along B. If the magnetic field is rotated around the Y axis through an angle θ_0 relative to the laboratory system then, by using the known formulas for the transformation of vector components upon rotation, we easily obtain for this case the connection between the polarization characteristic \tilde{I}^{Z-X} with the previously calculated I^{Z-X} :

$$\tilde{I}^{Z-X} = I^{Z-X} \cos 2\theta_0. \quad (15)$$

If the orientation of B relative to the laboratory system is arbitrary, the dependence of \tilde{I}^{Z-X} on the angles is somewhat more complicated: $\tilde{I}^{Z-X} = I^{Z-X} f(\psi, \theta, \varphi)$, where $f(\psi, \theta, \varphi)$ is a certain function obtained by rotation through the Euler angles $\psi, \theta,$ and φ .

2)We note in this connection that the use in [4] of a pure electron impact contour for convolution with the quasistatic contour leads to an incorrect asymptotic behavior of the intensity, see [14].

5. EXACT SOLUTION

Our problem, as already noted, can also be solved accurately, but this calls for laborious computer calculations^[4]. The solution method given in^[4] is based on a numerical solution of the secular equations followed by numerical integrations of the results with respect to the angle and with respect to the modulus of the field, with simultaneous convolution with the electron impact broadening. Naturally, in view of the high degree of degeneracy of the hydrogen levels, such an approach becomes extremely complicated with increasing *n*.

We wish to show here that even in the general formulation one can go much farther in the analytic solution of the problem than in^[4], and simplify by the same token the numerical calculations. To this end it is necessary to use the four-dimensional symmetry properties of the hydrogen atom, which enable us to get along without solving the secular equations, by choosing wave functions that diagonalize the Hamiltonian (see^[15]). These wave functions are of the form (see^[15])

$$\Psi_{n'n''} = \sum_{i_1, i_2} D_{n'i_1}^{(n-1)/2}(0, \alpha_1, 0) D_{n''i_2}^{(n-1)/2}(0, \alpha_2, 0) \Psi_{i_1, i_2} \quad (16)$$

where $\Psi_{i_1, i_2} \equiv \Psi_{n_1 n_2 m}$; $D_{n'i}^{(n-1)/2}$ is the Wigner function^[16]; $i_1 = 1/2(m + n_2 - n_1)$, $i_2 = 1/2(m + n_1 - n_2)$ are the quantum numbers of the projections of the vectors $\mathbf{J}_1 = (\hat{\mathbf{L}} - \hat{\mathbf{A}})/2$, $\mathbf{J}_2 = (\hat{\mathbf{L}} + \hat{\mathbf{A}})/2$ on the direction of \mathbf{F} ; n' and n'' are the quantum numbers of the projections of \mathbf{J}_1 and \mathbf{J}_2 respectively on the directions of $\boldsymbol{\omega}_1, \boldsymbol{\omega}_2 = \alpha e^{-1}\{\epsilon \mathbf{B} \pm \mathbf{F}\}$; $\hat{\mathbf{A}}$ is the Runge-Lenz vector^[12]

$$\alpha_1 = \arccos \frac{\mathbf{F} \boldsymbol{\omega}_1}{|\mathbf{F}| |\boldsymbol{\omega}_1|}, \quad \alpha_2 = \arccos \frac{\mathbf{F} \boldsymbol{\omega}_2}{|\mathbf{F}| |\boldsymbol{\omega}_2|}.$$

The eigenvalues of the energy take in the first approximation the form

$$\frac{\Delta E}{h} \approx n' |\boldsymbol{\omega}_1| + n'' |\boldsymbol{\omega}_2| = \frac{\alpha}{e} F_0 \beta \left[n' \left(1 - 2 \frac{\epsilon B}{F_0} \frac{n_B \beta}{\beta^2} + \frac{\epsilon^2 B^2}{F_0^2} \right)^{1/2} + n'' \left(1 + 2 \frac{\epsilon B}{F_0} \frac{n_B \beta}{\beta^2} + \frac{\epsilon^2 B^2}{F_0^2} \right)^{1/2} \right], \quad (17)$$

where $\boldsymbol{\beta} = \mathbf{F}/F_0$, $|\boldsymbol{\beta}| = \beta$, $n_B = \mathbf{B}/|\mathbf{B}|$. Then, substituting (16) and (17) in (3), we can easily verify that by virtue of the presence of the δ -function the integral with respect to the angular variables can be evaluated, and the expression for the profile of the line component reduces to a single integral with respect to the modulus of the field. The calculation of this integral, however, is still a difficult task, in view of the presence of a complicated dependence of the integrand on the sums with D-functions and can be performed only numerically.

The method described above, based on perturbation theory, also makes it possible, as noted, to get along without solving the secular equations, and leads, unlike the exact solution, to analytic results that are directly connected with the value of \mathbf{B} . These results, as we have verified, turn out to be valid in the regions of practical interest already at half the line width. The method developed here is therefore preferable for diagnostic purposes.

The authors are sincerely grateful to G. V. Sholin for useful advice and discussions during the work and to V. I. Kogan for a discussion of the results.

APPENDIX

For convenience in comparison with the results of^[4], we present expressions for the coefficients C_{lk}^{Z-X} ($l = 1, 2, 3$), obtained by substituting (5) and (6) in (3) and taking (7) into account, prior to averaging with respect to $\cos \theta \equiv \gamma$:

$$\begin{aligned} \frac{a_0'^2}{6} C_{1k}^{z-x} = & \left\langle \frac{\gamma^2(1-\gamma^2)}{2} \left\{ 2 \sum_{m \neq k} 3C_m^2(L_x)_{mk} [(d_x)_{0m}(d_x)_{k0}(L_x)_{mm} \right. \right. \\ & - (d_x)_{k0}(d_x)_{0m}(L_x)_{kk}] + \sum_{m \neq k} C_m^2 |(L_x)_{mk}|^2 [2|(d_x)_{m0}|^2 - |(d_x)_{0m}|^2] \\ & - 2[|(d_x)_{k0}|^2 - |(d_x)_{0k}|^2] + 2 \sum_{m \neq k} \sum_{n \neq k} C_{mn}(L_x)_{mn}(L_x)_{nk} [2(d_x)_{k0}(d_x)_{0m} \\ & - (d_x)_{m0}(d_x)_{0n}] \left. \right\} + 1/2(1-\gamma^2)^2 \left\{ \sum_{m \neq k} C_m^2 |(L_x)_{mk}|^2 [2|(d_x)_{0m}|^2 \right. \\ & - |(d_x)_{0m}|^2] - 2[|(d_x)_{k0}|^2 - |(d_x)_{0k}|^2] + 2 \sum_{m \neq k} \sum_{n \neq k} C_{mn}(L_x)_{mn}(L_x)_{nk} \\ & \times [2(d_x)_{k0}(d_x)_{0m} - (d_x)_{k0}(d_x)_{0m}] + \sum_{m \neq k} \sum_{n \neq k} C_{mn}(L_x)_{mk}(L_x)_{kn} \\ & \times [2(d_x)_{0n}(d_x)_{m0} - (d_x)_{0n}(d_x)_{m0}] \left. \right\} - 1/2(1-\gamma^2) \left\{ \sum_{m \neq k} C_m^2 |(L_x)_{mk}|^2 \right. \\ & \times [|(d_y)_{m0}|^2 - |(d_y)_{0m}|^2] + 2 \sum_{m \neq k} \sum_{n \neq k} C_{mn}(L_x)_{mk}(L_x)_{nk}(d_y)_{k0}(d_y)_{0m} \\ & \left. + \sum_{m \neq k} \sum_{n \neq k} C_{mn}(L_x)_{mk}(L_x)_{kn}(d_y)_{m0}(d_y)_{0n} \right\} \Bigg\rangle_{\gamma}, \quad (A.1) \end{aligned}$$

$$\begin{aligned} \frac{a_0'^2}{6} C_{2k}^{z-x} = & \left\langle \frac{\gamma^2(1-\gamma^2)}{2} \left\{ 6(L_x)_{kk}(d_x)_{0k} \sum_{m \neq k} C_m(L_x)_{mk}(d_x)_{m0} \right. \right. \\ & \left. \left. + [2|(d_x)_{k0}|^2 - |(d_x)_{0k}|^2] \left(\sum_m |(L_x)_{mk}|^2 C_m \right) \right\} \right. \\ & \left. + \frac{(1-\gamma^2)^2}{2} \left(\sum_m C_m |(L_x)_{mk}|^2 \right) [2|(d_x)_{k0}|^2 - |(d_x)_{0k}|^2] \right\rangle_{\gamma}, \quad (A.2) \end{aligned}$$

$$\frac{a_0'^2}{6} C_{3k}^{z-x} = \left\langle \frac{\gamma^2(3\gamma^2-1)}{4} (L_x)_{kk}^2 [|(d_x)_{k0}|^2 - |(d_x)_{0k}|^2] \right\rangle_{\gamma}, \quad (A.3)$$

$$C_{m,n} = \left(1 - \frac{q_{m,n}}{q_k} \right)^{-1}, \quad C_{m,n} = C_m C_n, \\ a_0'^2 = a_0^2 e^2 \frac{2^6 n^6 (n-1)^{2n-6}}{(n+1)^{2n+6}}$$

We note that both the components of the vectors \mathbf{L} and \mathbf{d} and the parabolic wave functions in these expressions are taken in the same coordinate system, which is connected with the field \mathbf{F} . The lower state is marked by the subscript 0.

After averaging with respect to γ ($\langle \dots \rangle_{\gamma}$) $\int_{-1}^{+1} \dots d\gamma$ and grouping like terms, the expressions (A.1)–(A.3) become much simpler. In the subsequent calculations, only one or two terms remain in the sums of (A.1)–(A.3) for the concrete cases of the lines $L_{\alpha'}$, L_{β} , etc. (cf. (10) and (11)), so that the determination of the numerical coefficients in (10) and (11) becomes quite simple.

¹Plasma Research Methods, ed. by Lohte-Holtgreven (Russ. transl.), Mir, 1970, p. 446.

²I. M. Podgorniy, *Lektsii po diagnostike plazmy* (Lectures on Plasma

Diagnostics), Atomizdat, 1968.

³I. I. Sobel'man, *Vvedenie v teoriyu atomnykh spektrov (Introduction to the Theory of Atomic Spectors)*, Fizmatgiz, 1963.

⁴Nguyen-Hoc, H. W. Drawin, and L. Herman, *J. Quant. Spectrosc. Radiat. Transfer* **7**, 429 (1967).

⁵G. V. Sholin, *Dokl. Akad. Nauk SSSR* **175**, 1256 (1967) [*Sov. Phys.-Dokl.* **12**, 811 (1968)].

⁶G. V. Sholin, *Opt. Spektrosk.* **26**, 489 (1969).

⁷W. L. Wiese, *Proc. of the X Int. Conf. Phenom. Ionized Gases*, London, 1971.

⁸E. K. Zavoiskii, Yu. T. Kalinin, V. A. Skoryupin, V. V. Shapkin, and G. V. Sholin, *Zh. Eksp. Teor. Fiz. Pis'ma Red.* **13**, 19 (1971) [*JETP Lett.* **13**, 12 (1971)].

⁹H. Goldstein, *Classical Mechanics*, Addison-Wesley, 1950.

¹⁰I. M. Gel'fand and G. E. Shilov, *Obobshchennye funktsii i deistviya nad nimi*, Vol. 1, Fizmatgiz, 1959 [*Generalized Functions*, Vol. 1, Academic, 1963].

¹¹J. Holtzmark, *Ann. Phys. (Leipz.)* **58**, 577 (1919).

¹²J. W. B. Hughes, *Proc. Phys. Soc. Lond.* **91**, 810 (1967).

¹³H. A. Bethe and E. E. Salpeter, *Quantum Mechanics of One- and Two-electron Atoms*, Academic, 1957.

¹⁴H. Griem, *Phys. Rev. A* **140**, 1140 (1965).

¹⁵Yu. N. Demkov, B. S. Monozon, and V. N. Ostrovskii, *Zh. Eksp. Teor. Fiz.* **57**, 1431 (1969) [*Sov. Phys.-JETP* **30**, 775 (1970)].

¹⁶E. P. Wigner, *Group Theory*, Academic, 1959.

Translated by J. G. Adashko

251